Shapes coexistence in the frame of the Bohr model

Petrică Buganu, Radu Budaca, Andreea Budaca

Seminar in cadrul Departementului de Fizică Teoretică, IFIN-HH

1. R. Budaca, P. Buganu, A. I. Budaca, Phys. Lett. B 776 (2018) 26 – 31.
2. R. Budaca, A. I. Budaca, EPL 123 (2018) 42001.
3. R. Budaca, P. Buganu, A. I. Budaca, Nucl. Phys. A (2019) in press.

PN-III-P1-1.1-TE-2016-0268, Director proiect: Radu Budaca

1. *38th International Workshop on Nuclear Theory*, Rila Mountains, Bulgaria, 23 – 29 June, 2019.
2. *International Conference on Shapes and Symmetries in Nuclei: From experiment to Theory*, 5 – 9 November, 2018, Gif sur Yvette, France.
3. *The International Conference on Nuclear Structure and Related Topics*, 3 – 9 June, 2018, Burgas, Bulgaria.
4. *9th International Workshop on Quantum Phase Transitions in Nuclei and Many – Body Systems*, 22 – 25 May, 2018, Padova, Italy.

Content

- Introduction in the field of nuclear shape phase transitions
- Motivation for the present study
- Bohr Hamiltonian with a sextic oscillator potential
- The critical point of the phase transition from spherical vibrator [U(5)] to prolate rotor [SU(3)] and the shape coexistence phenomenon
- Conclusions

Bohr-Mottelson Collective Model

A. Bohr, Mat. Fyz. Medd. K. Dan. Vidensk. Selsk. 26 (1952) No. 14.
A. Bohr, B. R. Mottelson, Mat. Fys. Medd. K. Dan. Vidensk. Selsk. 27 (1953) No. 16.

The excitation spectra of the nuclei are interpreted as vibrations and rotations of their surface:

$$R(\theta,\varphi,t) = R_0 \left[1 + \sum_{\lambda=0}^{\infty} \sum_{\mu=-\lambda}^{\lambda} \alpha^{*}_{\lambda\mu}(t)\, Y_{\lambda\mu}(\theta,\varphi) \right]$$

R_0 – radius of spherical nucleus, $\alpha_{\lambda\mu}$ – surface collective coordinates, $Y_{\lambda\mu}(\theta,\varphi)$ – spherical harmonics.

Types of multipole deformations:

$\lambda = 0$ $\lambda = 1$ $\lambda = 2$ $\lambda = 3$ $\lambda = 4$

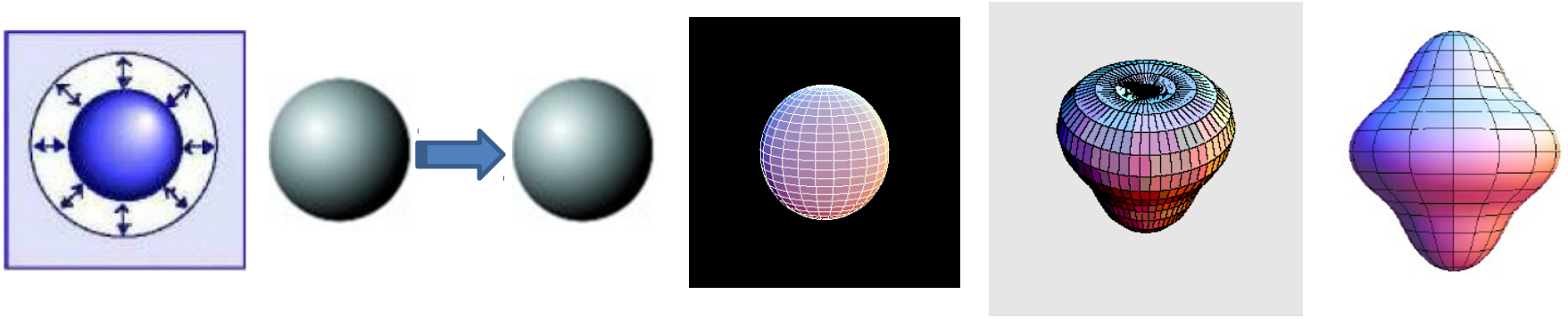

monopole dipole quadrupole octupole hexadecupole

Quadrupole deformation: Wigner function

$$I_{Lab} \xrightarrow{R(\Omega)} I_{Int}: \quad a_{2\mu} = \sum_{\mu'} D^{2}_{\mu'\mu}(\Omega)\, \alpha_{2\mu}; \quad \Omega \equiv (\theta_1, \theta_2, \theta_3)$$ Euler angles

Bohr-Mottelson transformation (intrinsic reference frame):

$$a_{20} = \beta\cos\gamma, \; a_{2,+2} = a_{2,-2} = \frac{\beta}{\sqrt{2}}\sin\gamma, \; a_{2,-1} = a_{2,+1} = 0; \; \beta > 0 \;\&\; \gamma \in [0, 2\pi].$$

$$\Delta R_k \equiv R_k - R_0 = R_0\sqrt{\frac{5}{4\pi}}\beta\cos\left(\gamma - \frac{2\pi}{3}k\right) \quad k = 1,2,3.$$

$\beta = 0$ ⇒ spherical shape

$\beta > 0$ ⇒ deformed shape

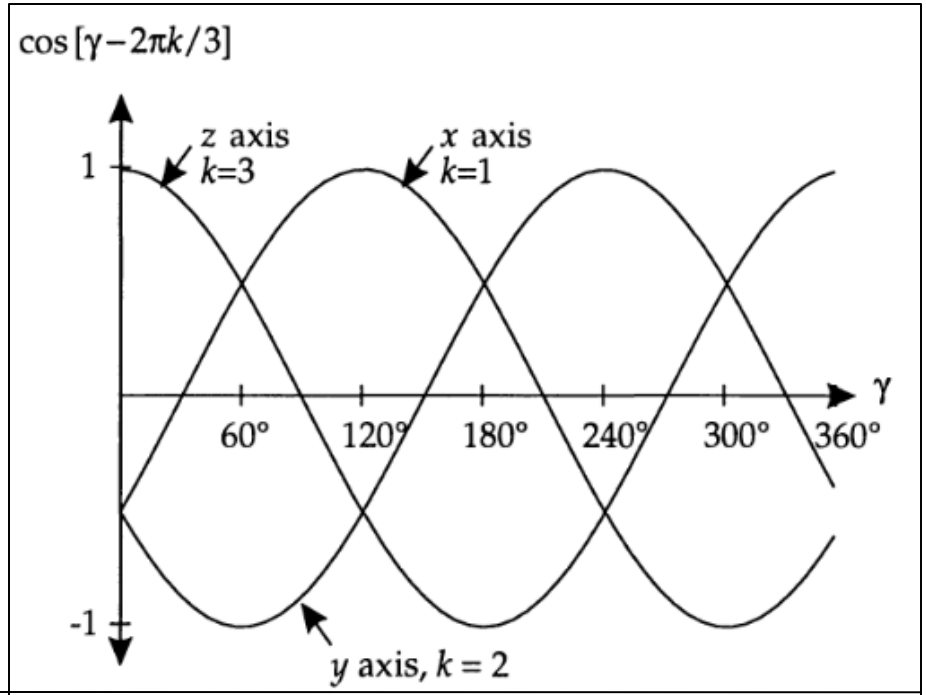

The stretching of the nuclear axis. W. Greiner, J. A. Maruhn, Nuclear Models, Springer-Verlag Berlin Heidelberg (1996).

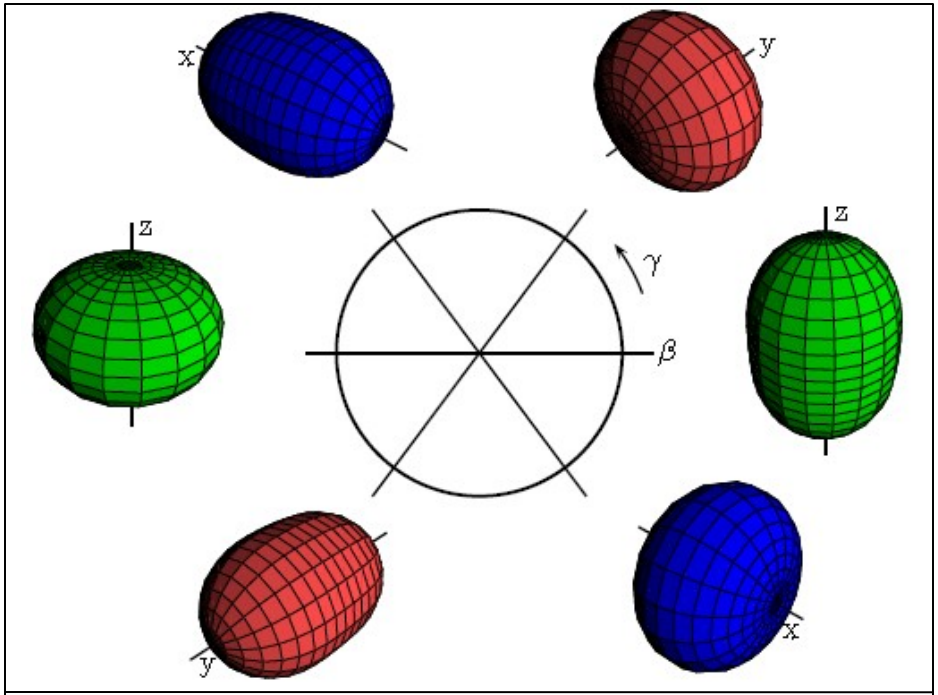

β=0.4 and γ=nπ/3 (n=0,1,2,3,4,5.): prolate(n=0,2,4), oblate (n=1,3,5) and triaxial in rest. L. Fortunato, Eur. Phys. J. A 26 (2005) 1-30.

The Bohr-Mottelson Hamiltonian:

$$H\psi(\beta,\gamma,\theta_1,\theta_2,\theta_3) = E\psi(\beta,\gamma,\theta_1,\theta_2,\theta_3)$$

$$H = -\frac{\hbar^2}{2B}\left[\frac{1}{\beta^4}\frac{\partial}{\partial\beta}\beta^4\frac{\partial}{\partial\beta} + \frac{1}{\beta^2\sin 3\gamma}\frac{\partial}{\partial\gamma}\sin 3\gamma\frac{\partial}{\partial\gamma}\right] + \frac{\hbar^2}{8B}\sum_{k=1}^{3}\frac{Q_k^2}{\beta^2\sin^2\left(\gamma - \frac{2\pi}{3}k\right)} + V(\beta,\gamma)$$

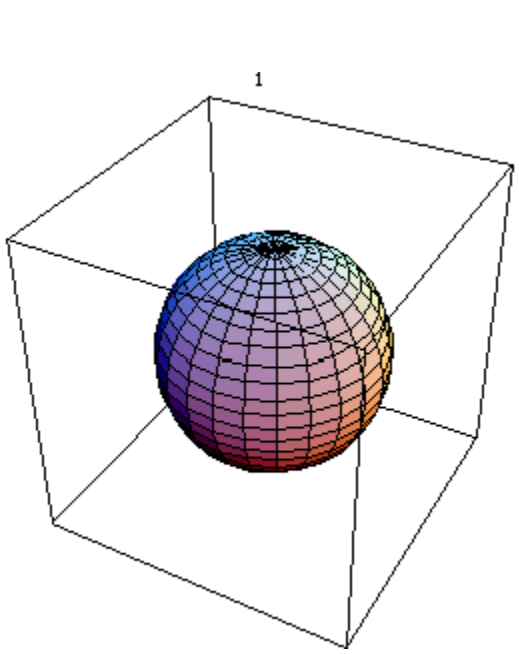

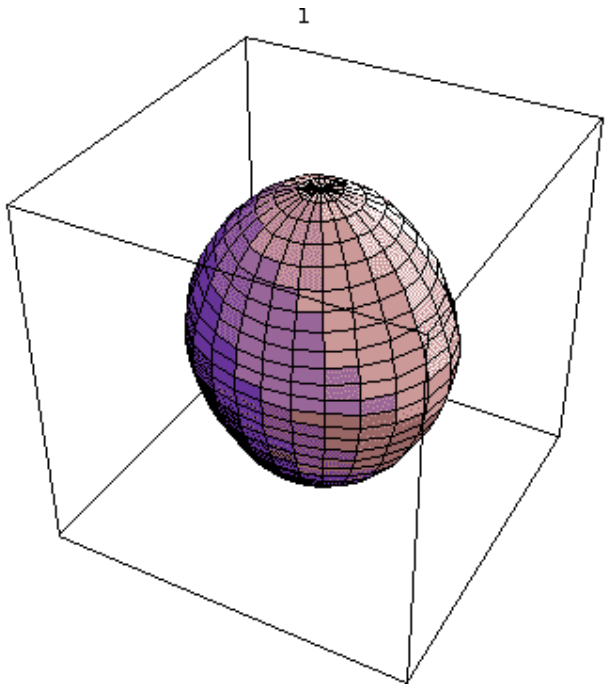

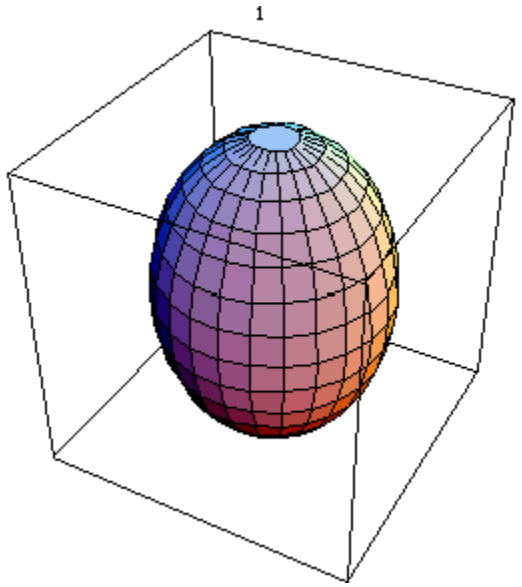

H = β vibration + γ vibration + rotation + potential

Reviewed solutions of the Bohr-Mottelson Hamiltonian in:

L. Fortunato, Eur. Phys. J. A 26 (2005) 1.

P. Buganu, L. Fortunato, J. Phys. G: Nucl. Part. Phys. 43 (2016) 093003.

Separable potentials: $V(\beta,\gamma) = V_1(\beta) + \frac{V_2(\gamma)}{\beta^2}$

Two differential equations, one for β and other for γ and the Euler angles:

$$\frac{1}{\beta^4}\frac{\partial}{\partial\beta}\beta^4\frac{\partial}{\partial\beta} + \frac{\omega}{\beta^2} + u_1(\beta)\Big]\xi(\beta) = \varepsilon\xi(\beta),\ \ u_1(\beta) = \frac{2B}{\hbar^2}V_1(\beta),\ \ \varepsilon = \frac{2B}{\hbar^2}E,\ \ \omega \text{ separation constant}$$

$$\frac{1}{\sin 3\gamma}\frac{\partial}{\partial\gamma}\sin 3\gamma\frac{\partial}{\partial\gamma} + \sum_{k=1}^{3}\frac{\hat{Q}_k^2}{4\beta^2\sin^2\left(\gamma - \frac{2\pi}{3}k\right)} + u_2(\gamma)\Big]\phi(\gamma,\theta_1,\theta_2,\theta_3) = \omega\phi(\gamma,\theta_1,\theta_2,\theta_3),\ \ u_2(\gamma) = \frac{2B}{\hbar^2}V_2(\gamma)$$

Potentials of frequent use for β

Name	Parameterization	Notes
Harmonic Oscillator	$\frac{1}{2}C\beta^2$	ES
Davidson	$\frac{1}{2}C\beta^2 + \frac{B}{\beta^2}$	ES
Square well	$\begin{cases}0 & \beta < \beta_w\\ \infty & \beta > \beta_w\end{cases}$	ES
Coulomb	$\frac{A}{\beta}$	ES
Kratzer	$\frac{A}{\beta} + \frac{B}{\beta^2}$	ES
quartic	$A\beta^4$	NES
Sextic	$A\beta^6 + B\beta^4 + C\beta^2$	QES
Morse	$e^{-2A(\beta-\beta_0)} - 2e^{-A(\beta-\beta_0)}$	QES
Displaced harmonic	$\frac{1}{2}C(\gamma-\gamma_0)^2$	Aperiodic
Cosine	$A\cos(3\gamma) + B\cos^2(3\gamma)$	Periodic
Inverse sine square	$\frac{\mu}{\sin^2(3\gamma)}$	Periodic

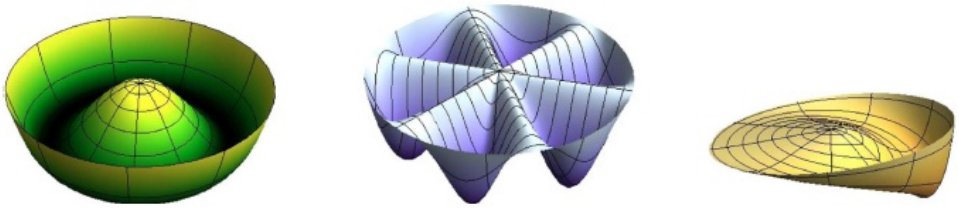

Plot of champagne bottle, plastic bottle and sea-shell potentials, that are examples of γ–unstable, γ-stable and localized γ-stable potentials, respectively.

Other classification of these solutions in soft and rigid solutions, respectively. In the rigid case, a variable is set to a given value β_0 or γ_0. The wave functions and the quantum fluctuations in that variable are disregarded.

P. Buganu, L. Fortunato, J. Phys. G: Nucl. Part. Phys. 43 (2016) 093003.

The Interacting Boson Approximation (IBA)

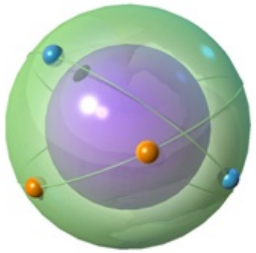

F. Iachello, A. Arima, *The Interacting Boson Model*, Cambridge, England, University Press, Cambridge, 1987.

The IBA describes even – even nuclei in terms of interacting valence nucleon pairs with angular momenta L= 0 (s bosons) and 2 (d bosons):

$$s^+ \Leftrightarrow \hat{S}^+ \equiv \sum_j \alpha_j \left(a_j^+ \times a_j^+\right)_0^{(0)}, \quad d_\mu^+ \Leftrightarrow \hat{D}_\mu^+ \equiv \sum_{jj'} \beta_{jj'} \left(a_j^+ \times a_{j'}^+\right)_\mu^{(2)} \qquad \left[\hat{S}, \hat{S}^+\right] = 1 - \frac{\hat{n}}{\Omega} \approx 1 \text{ while } \left[s, s^+\right] = 1$$

The IBA is a truncation and a subsequent bosonization of the Shell Model in terms of *S* and *D* pairs, while In the classical limit ($N \to \infty$) the expectation value of the IBA Hamiltonian between coherent states reduces to the Bohr Hamiltonian.

A standard two – dimensional parametrization of the IBA Hamiltonian is:

$$\hat{H}(N, \eta, \chi) = a(\eta\, \hat{n}_d + \frac{\eta - 1}{N} \hat{Q}_\chi \cdot \hat{Q}_\chi)$$

d – boson number operator $n_d = d^+ \cdot \tilde{d} \qquad \tilde{d}_\mu = (-1)^{2-\mu} d_{-\mu}$

quadrupole operator $\hat{Q}_\chi = (s^\dagger \tilde{d} + d^\dagger s)^{(2)} + \chi [d^\dagger \times \tilde{d}]^{(2)}$

N – total number of bosons; a = 1 MeV – scaling factor; η and χ – dimensionless control parameters

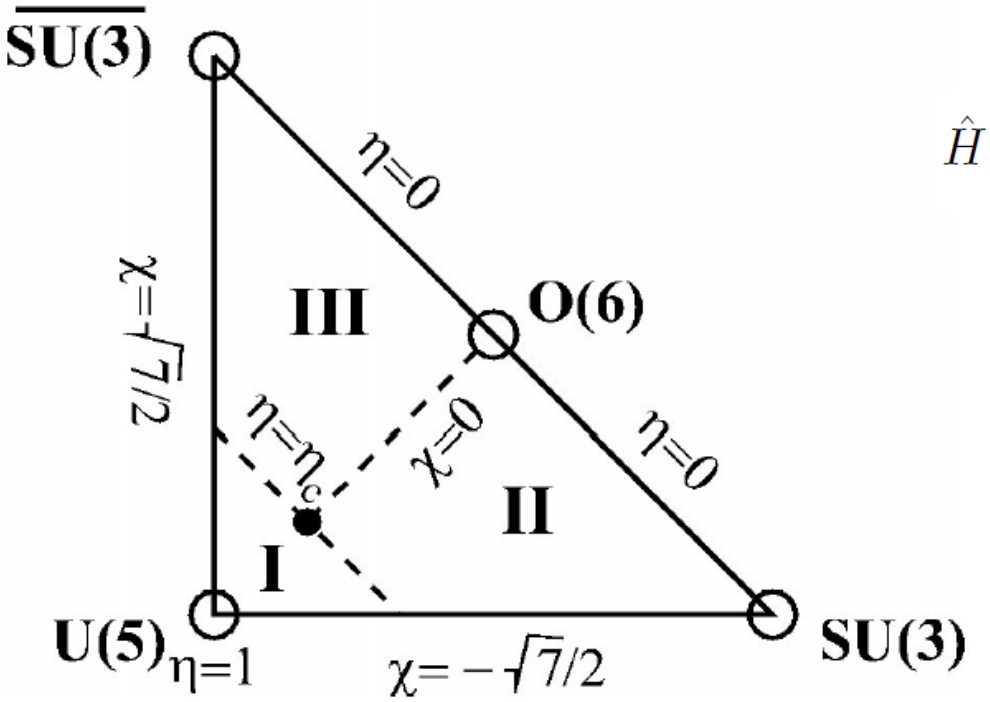

$$\hat{H}(N,\eta,\chi) = a(\eta\,\hat{n}_d + \frac{\eta-1}{N}\,\hat{Q}_\chi\cdot\hat{Q}_\chi)$$

$\eta = 1$, $\chi = 0$: U(5) (spherical shape)
$\eta = 0$, $\chi = -\sqrt{7}/2$: SU(3) (prolate shape)
$\eta = 0$, $\chi = +\sqrt{7}/2$: SU(3) (oblate shape)
$\eta = 0$, $\chi = 0$: O(6) (γ – unstable shape)

FIGURE 1. The extended Casten triangle [12] and its different phases. The solid dot in the center represents the second-order transition between spherical nuclei (Phase I) and deformed nuclei with prolate (Phase II) and oblate (Phase III) forms. The dashed lines correspond to first-order phase transitions.

J. Jolie, R. F. Casten, P. von Brentano, and V. Werner, Phys. Rev. Lett. 87 (2001) 162501.
J. Jolie, S. Heinze, P. Cejnar, Revista Mexicana de Fisica 49 (2003) 29 – 33.

The geometric interpretation of the IBA Hamiltonian can be derived by using *s* and *d* – boson condensate states [R. Gilmore, J. Math. Phys. 20 (1979) 891; J. N. Ghinocchio, M. W. Kirson, Phys. Rev. Lett. 44 (1980) 1744]:

$$|N,\beta,\gamma\rangle = \frac{1}{\sqrt{N!}}\left(b_c^\dagger\right)^n|0\rangle;\ b_c^\dagger = \frac{1}{\sqrt{1+\beta^2}}\left[s^\dagger + \beta\cos\gamma d_0^\dagger + \frac{1}{\sqrt{2}}\beta\sin\gamma\left(d_2^\dagger + d_{-2}^\dagger\right)\right]$$

Energy functional $E(N,\eta,\chi;\beta,\gamma)=\langle N,\beta,\gamma|H(N,\eta,\chi)|N,\beta,\gamma\rangle$

$$E(N,\eta,\chi;\beta,\gamma)=\frac{1}{(1+\beta^2)^2}\left\{[N\eta-(1-\eta)(4N+\chi^2-8)]\beta^2+4(N-1)(1-\eta)\sqrt{\frac{2}{7}}\chi^3\cos 3\gamma\right\}+$$
$$\frac{1}{(1+\beta^2)^2}\left\{\left[N\eta-(1-\eta)\left(\frac{2N+5}{7}\chi^2-4\right)\right]\beta^4\right\}$$

Analogy to the Landau theory

Instead of the thermodynamic potential $\phi(P,T;\xi)$, that depends on external parameters (pressure *P* and Temperature *T*) and the order parameter ξ, one has the energy surface $E(N,\eta,\chi;\beta,\gamma)$ depending on external parameters η and χ and on the order parameters β and γ. The external parameters are related here to the number of valence and hence indirectly to the underlying shell structure.

The ground state energy obtained from the global minimum of the energy functional $E(N,\eta,\chi;\beta_0,\gamma_0)$ must be a continuous function of η and χ, similarly as the thermodynamic potential in the equilibrium configuration ξ_0 is a continuous function in *P* and *T*. Discontinuities in the first or second derivatives of $E(N,\eta,\chi;\beta_0,\gamma_0)$ with respect to the control parameters result in first – or second – order shape phase transition.

J. Jolie, S. Heinze, P. Cejnar, Revista Mexicana de Fisica 49 (2003) 29 – 33.

Motivation for the present study

R. F. Casten, Nature Physics 2 (2006) 811.

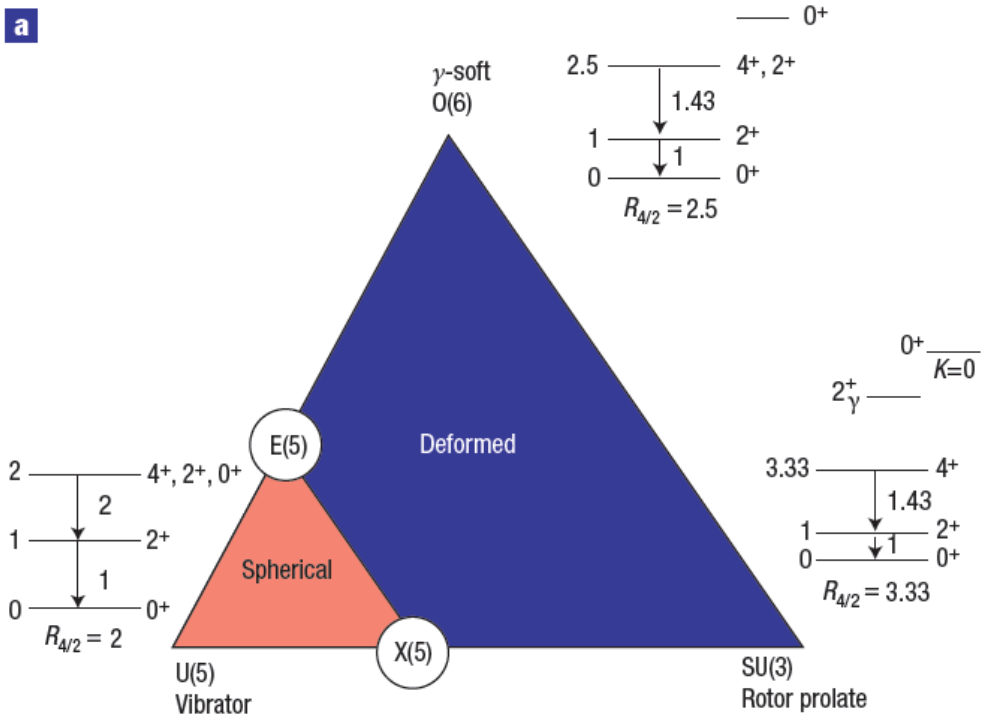

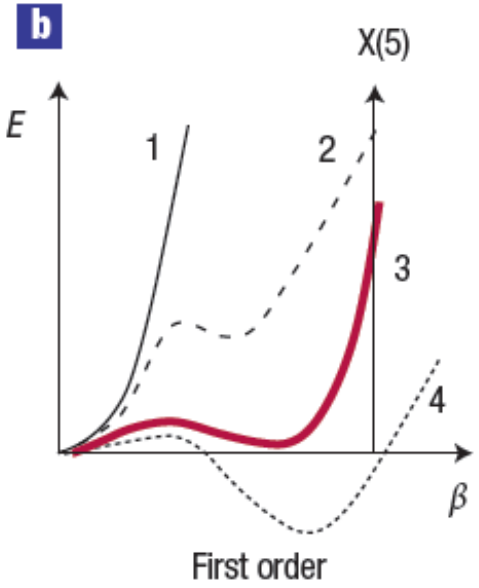

Fig. 3b, for a first-order transition, a coexisting, deformed minimum appears (curve 2) as an excited configuration. With increasing valence nucleon number, its energy decreases, eventually becoming the equilibrium shape (curve 4). The point of degeneracy (curve 3) of the coexisting shapes is the critical point.

Figure 1 Symmetry triangle for nuclear structure. **a**, showing the traditional paradigms at the vertices (along with mini-level schemes), and the two critical point symmetries, E(5) and X(5), at the termini of the phase-transitional region between spherical and deformed nuclei. Note that there are two systems for labelling these paradigms: the geometric language of vibrator, rotor, γ-soft, E(5), and X(5), which are solutions to the Bohr hamiltonian, and symmetry-based labels from the IBA (U(5), SU(3) and O(6)). This distinction should be borne in mind and is the reason, for example, that E(5) and X(5) are shown in open circles, to distinguish them from the dynamical symmetries at the vertices. Also, even solutions such as U(5) and the vibrator, which appear in both algebraic and geometric approaches, although similar, are not identical.

Interacting Boson Approximation (IBA): F. Iachello, A. Arima, *The Interacting Boson Model*, Cambridge University Press, Cambridge, 1987.
Bohr – Mottelson Geometrical Model: A. Bohr, Mat. Fys. Medd. K. Dan. Vidensk. Selsk. 26 (1952) No. 14;
A. Bohr, B. R. Mottelson, Mat. Fys. Medd. K. Dan. Vidensk. Selsk. 27 (1953) No. 16.

Bohr Hamiltonian with a sextic potential having simultaneous spherical and deformed minima

Radial-like differential equation for the β variable for prolate deformed nuclei is:
[F. Iachello, Phys. Rev. Lett. 87 (2001) 052502]

$$\left[-\frac{1}{\beta^4}\frac{\partial}{\partial\beta}\beta^4\frac{\partial}{\partial\beta}+\frac{L(L+1)}{3\beta^2}+v(\beta)\right]\Psi(\beta)=\epsilon^{\beta}\Psi(\beta).$$

A general sextic potential is used to introduce the barrier separating the two minima:
$v(\beta)=a\beta^2+b\beta^4+c\beta^6$

R. Budaca, P. Buganu, A. I. Budaca, Phys. Lett. B 776 (2018) 26 – 31. R. Budaca, A. I. Budaca, EPL 123 (2018) 42001.

The eigenvalue can be scaled as follows: $\epsilon^{\beta}(a,b,c)=a^{1/2}\epsilon^{\beta}(1,ba^{-3/2},ca^{-2})$

Due to the scaling property, one can start from the beginning with a potential of the form: $v(\beta)=\beta^2+a\beta^4+b\beta^6$

Making the change of function $\Psi(\beta)=\beta^{-2}\psi(\beta)$, one obtains a new form for the β equation:

$$\left[-\frac{\partial^2}{\partial\beta^2}+\frac{L(L+1)}{3\beta^2}+v_{eff}(\beta)\right]\psi(\beta)=\varepsilon^{\beta}\psi(\beta) \qquad v_{eff}(\beta)=\frac{2}{\beta^2}+\beta^2+a\beta^4+b\beta^6$$

The energies and the wave functions are obtained by numerical diagonalization using as a basis the solutions of the same equation but for an infinite square well potential:

$$\Psi_{vn}(\beta)=\frac{\sqrt{2}\beta^{-\frac{3}{2}}J_v\left(\frac{\alpha_n\beta}{\beta_W}\right)}{\beta_W J_{v+1}(\alpha_n)},\quad v=\sqrt{\frac{L(L+1)}{3}+\frac{9}{4}},\ \text{for } v(\beta)=\begin{cases}0, & \beta<\beta_W\\ \infty, & \beta>\beta_W\end{cases}$$

Jν are Bessel functions of the first kind, while α_n are their zeros associated to the boundary conditions for a suitably chosen limiting value β_w, which encompass the relevant part of the sextic potential. The boundary value β_w is fixed such that to achieve a satisfactory convergence (10^{-7}) for all considered energy states for a given dimension of the diagonalization basis (n=20).

In this study, the parameters *a* and *b,* describing the potential, are fixed such that the two minima, separated by a barrier, to have the same minimum energy.

$$v_{eff}(\beta) = \frac{2}{\beta^2} + \beta^2 + a\beta^4 + b\beta^6$$

$$v(\beta) = \beta^2 + a\beta^4 + b\beta^6$$

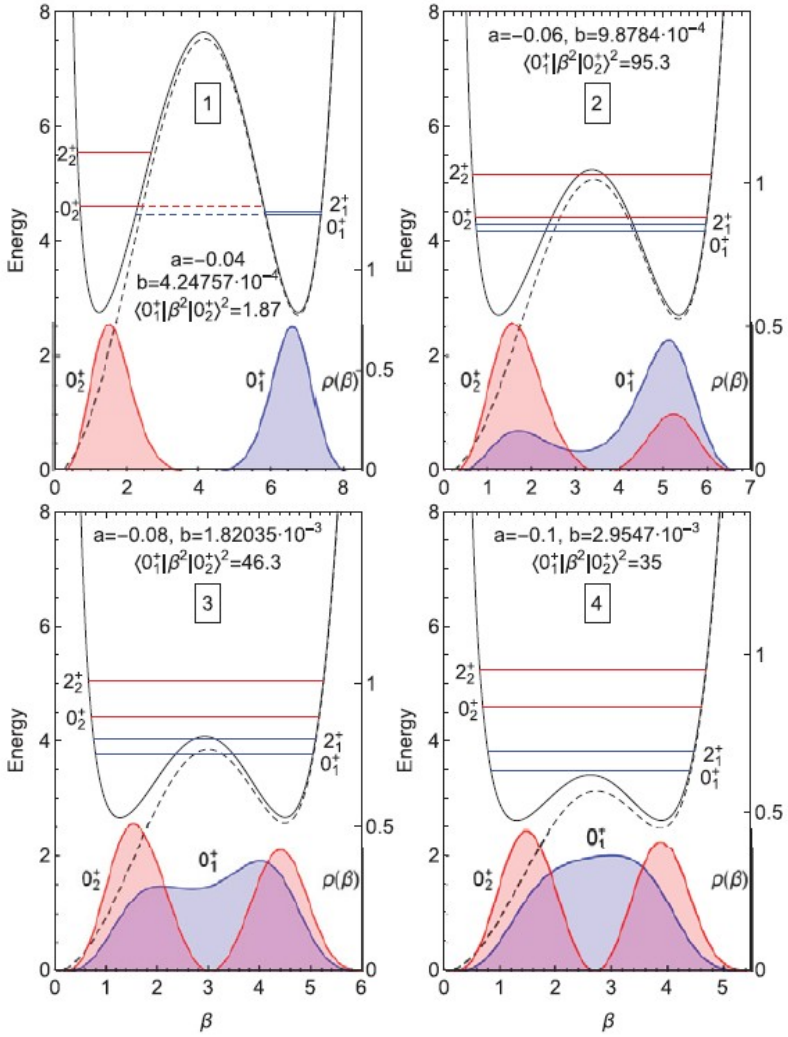

X(5).

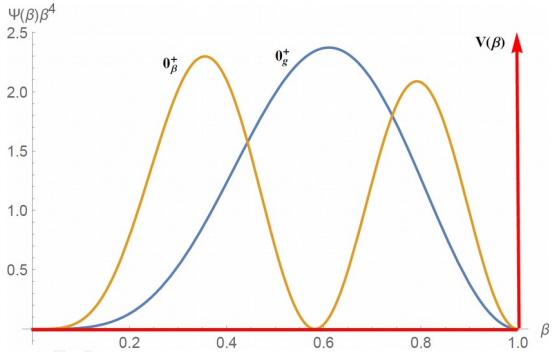

Fig. 1: (Colour online) Effective (solid) and original (dashed) collective potentials as well as the probability distribution corresponding to the first two β excited states are plotted as a function of β. The energy levels 0^+ and 2^+ belonging to the ground band and β excited band are shown using the same arbitrary units of the potential curves.

R. Budaca, A. I. Budaca, EPL 123 (2018) 42001.
R. Budaca, P. Buganu, A. I. Budaca, Phys. Lett. B 776 (2018) 26 – 31.

Th. Exp.

$\rho(E0) = 87.14 \cdot 10^{-3}$ $79(11) \cdot 10^{-3}$

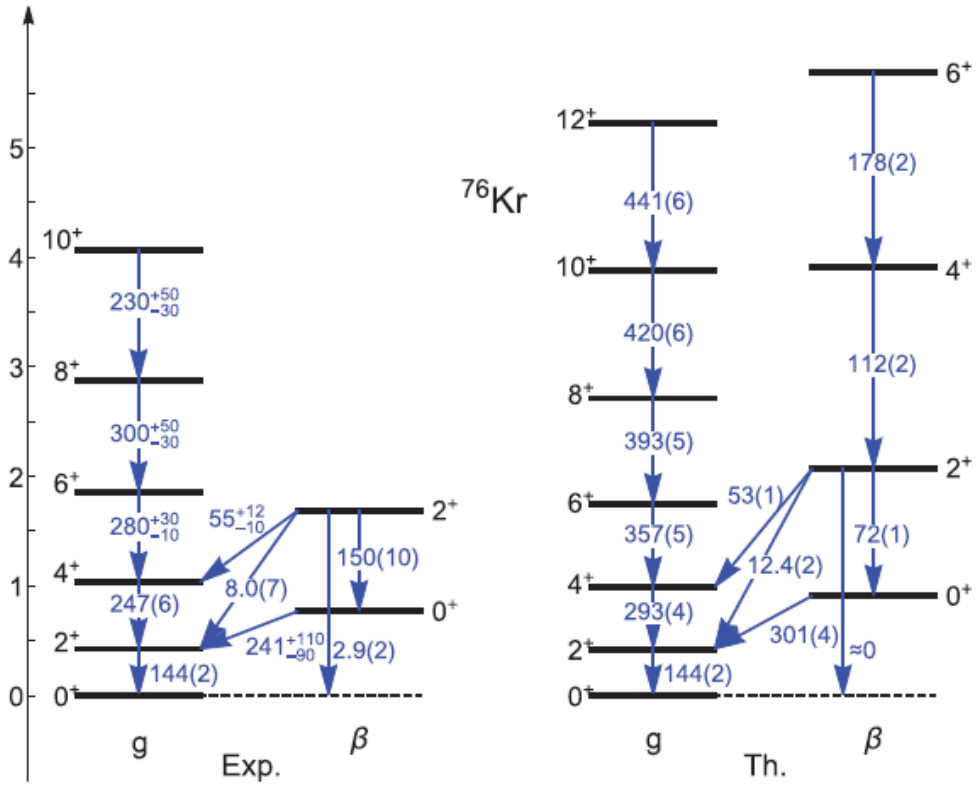

Fig. 3: (Colour online) Theoretical and experimental [18] energy spectra for ^{76}Kr including only $K^\pi = 0^+$ states. The energy scale of theoretical predictions is fixed to reproduce the experimental energy of 2_1^+ state, while the theoretical $B(E2)$ values are scaled to the experimental value of the $2_1^+ \rightarrow 0_1^+$ transition. Energy levels are given in Mev and $B(E2)$ values in e^2b^2.

R. Budaca, A. I. Budaca, EPL 123 (2018) 42001..

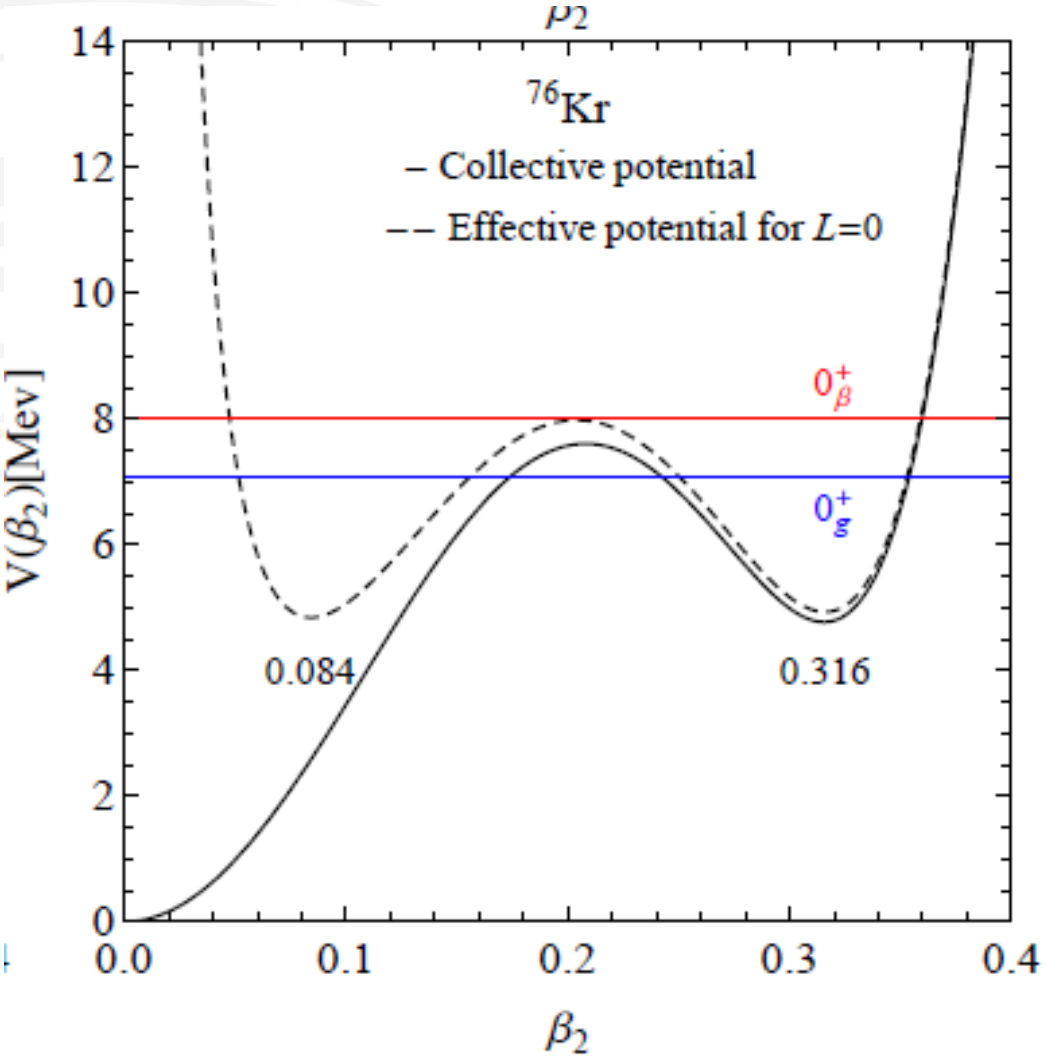

$$a = -0.07314 \text{ and } b = 1.5062 \cdot 10^{-3}$$

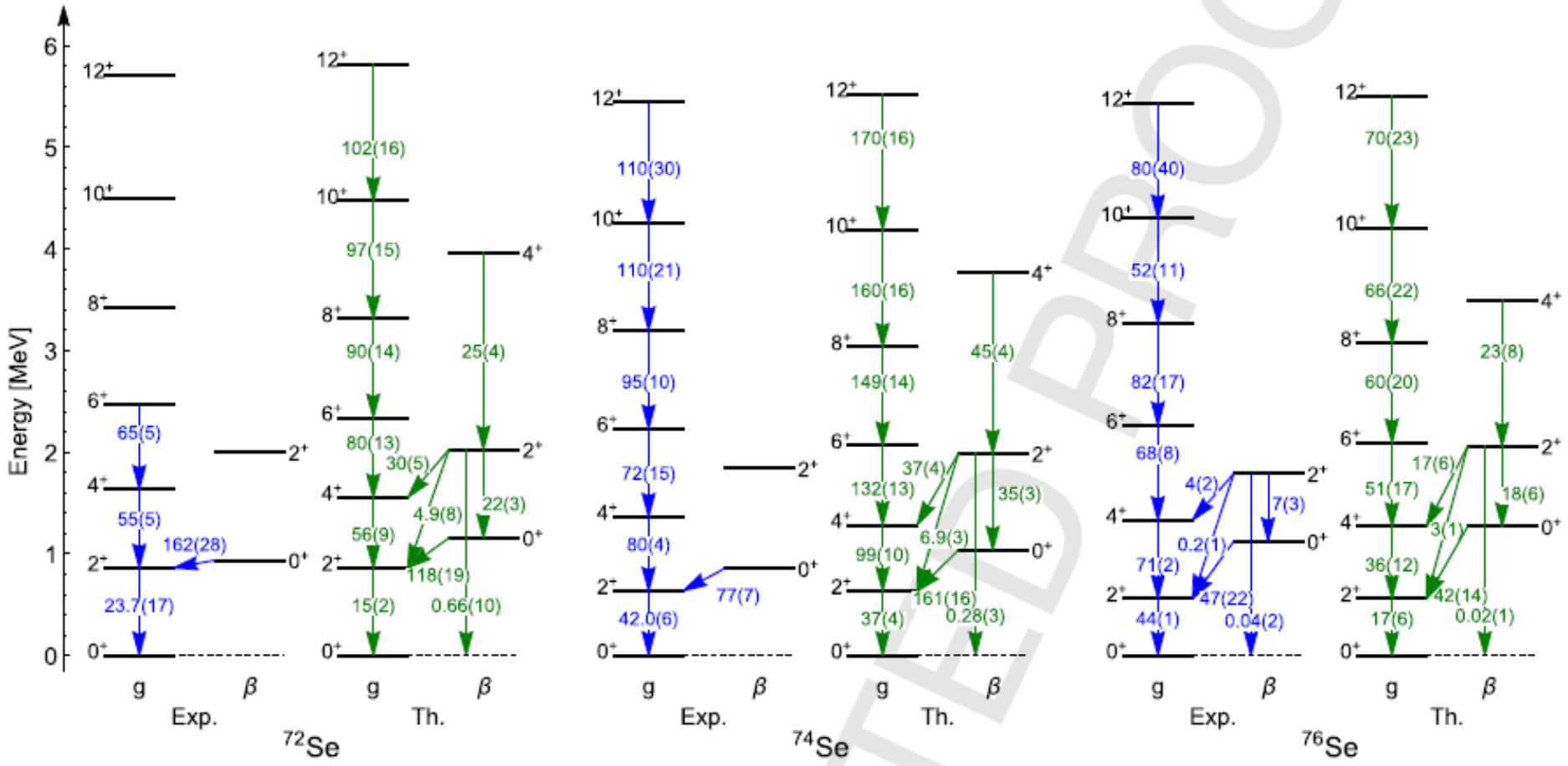

Fig. 1. Theoretical results are compared with experimental data for ground and β excited band energies and the associated $E2$ transition probabilities, given in MeV and respectively W.u., for ^{72}Se [40], ^{74}Se [41] and ^{76}Se [42].

R. Budaca, P. Buganu, A. I. Budaca, Nucl. Phys. A (2019) in press.

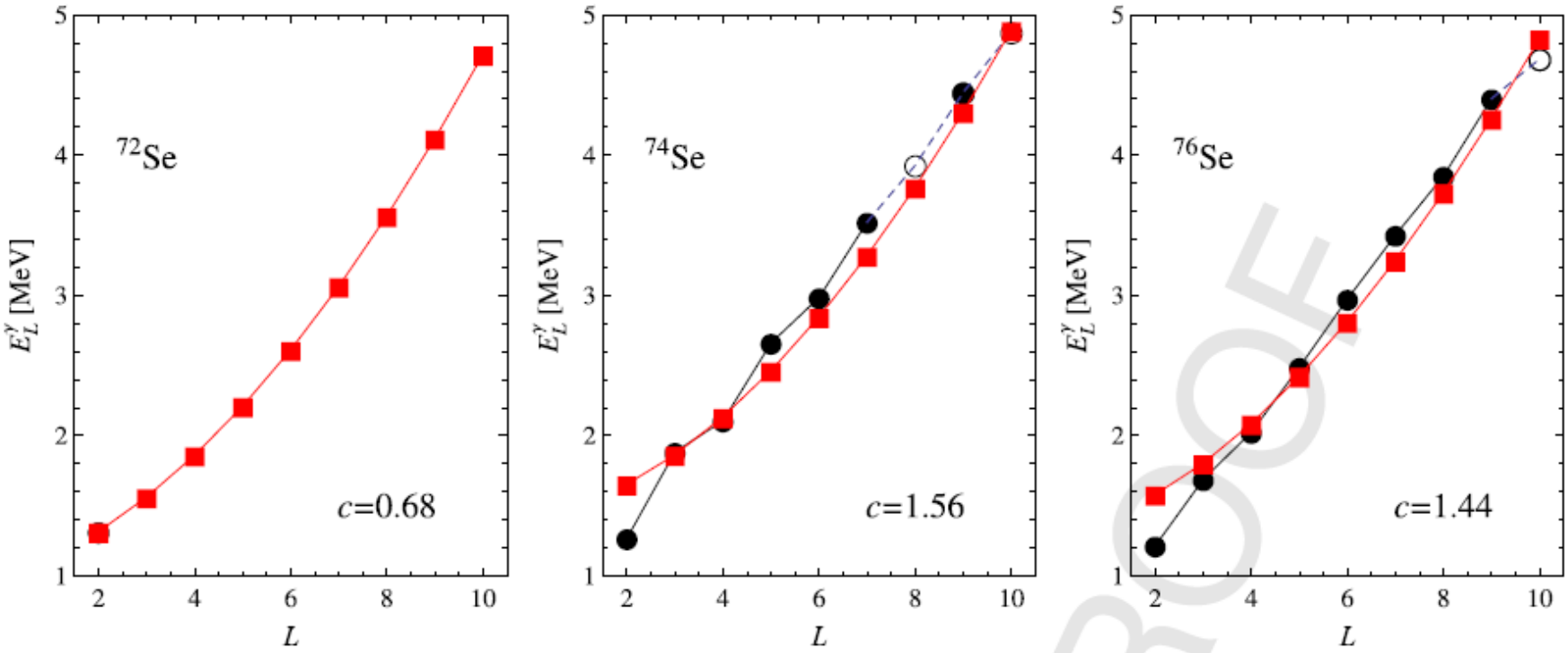

Fig. 2. Calculated (squares) and experimental (circles) absolute energy of the γ band levels as a function of angular momentum.

R. Budaca, P. Buganu, A. I. Budaca, Nucl. Phys. A (2019) in press.

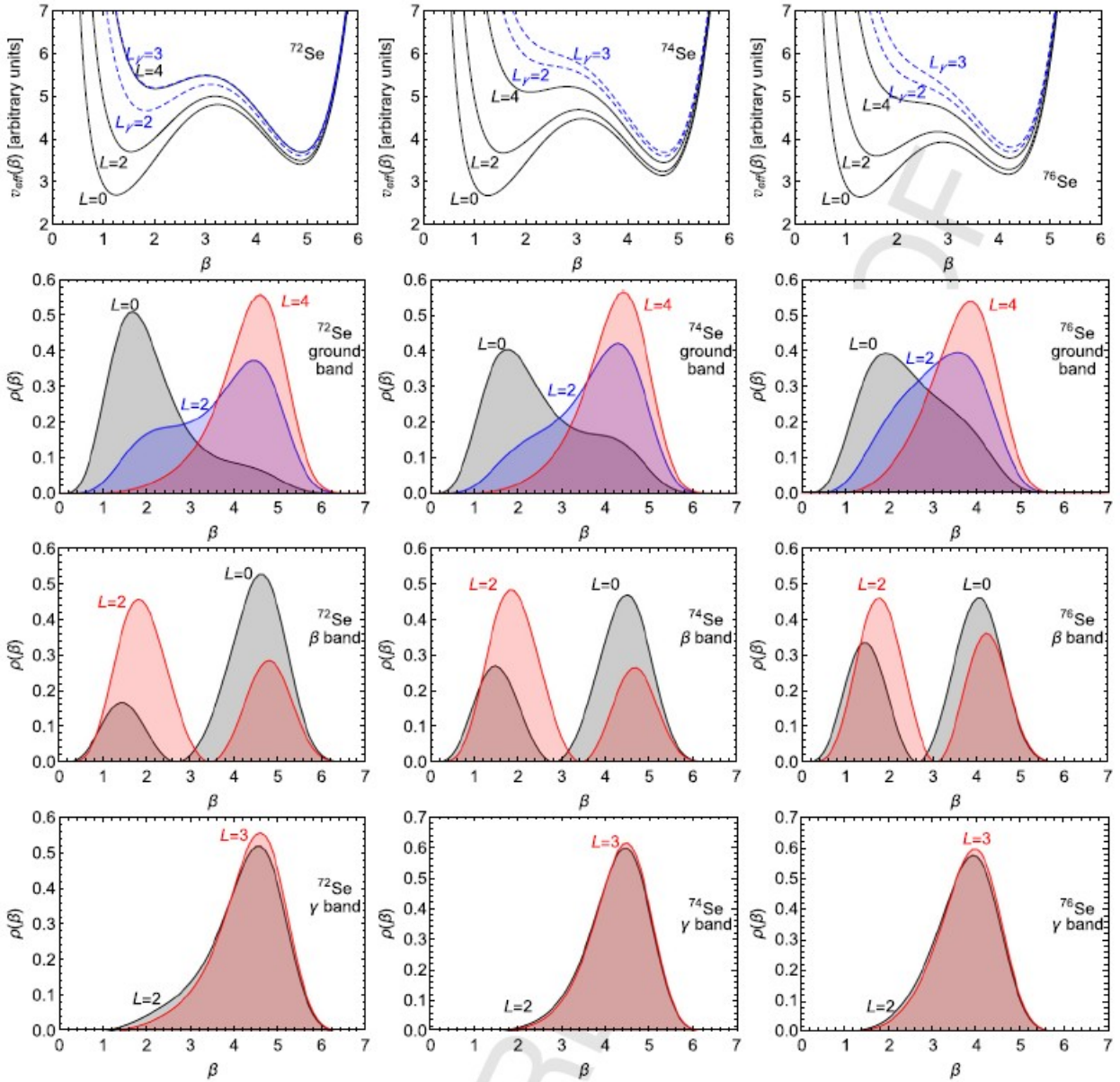

Fig. 4. Theoretical effective potentials (14) as well as the probability distribution corresponding to the $L = 0, 2, 4$ ground band states, $L = 0, 2$ β excited band states and $L = 2, 3$ γ band states are plotted as a function of β deformation for the ^{72,74,76}Se nuclei.

R. Budaca, P. Buganu, A. I. Budaca, Nucl. Phys. A (2019) in press.

Conclusions

- The influence had by the barrier for the critical point of the phase transition from spherical vibrator to axial rotor is investigated in the frame of the Bohr-Mottelson model using a sextic potential for the β variable. Moreover, the study goes beyond this particular situation by increasing considerably the height of the barrier.
- The parameters, describing the associated effective potential, are fixed such that the two minima, separated by barrier, to have the same minimum energy.
- The Hamiltonian is diagonalized in a basis of Bessel functions of the first kind, which in turn are solutions for the same problem but for an infinite square well potential.
- Analyzing the density distribution probabilities for the ground state and for the first 0^+ excited state, but also the monopole transition matrix element between these two states, one can see how the barrier influence dramatically the deformation of the ground and excited states and moreover, the fact that these states could present shape coexistence, coexistence with mixing and fluctuations, respectively, depending on the height of the barrier.
- Experimental realization of the present model is found for ^{76}Kr and ^{72,74,76}Se.